Supplementary material 1 Description of clinical manifestations during application of the Karanahan technology

Patient 1.

Date of birth: December 28, 1960

Medical history

2018 – Left-sided breast cancer was verified.

October 17, 2018 – Radical sector resection of the left breast

Histological examination: grade 2 infiltrating ductal carcinoma without lymphovascular invasion. No tumor spread to lymph nodes.

Immunohistochemical examination: ER 8, PR 6, HER2/neu 0, Ki67 20%

2019 – Local recurrence and progression of the disease

September 10, 2019 – Ultrasonography: a solid neoplasm sized 3.5*2.5*1 cm, with a distinct rugged contour, is detected subcutaneously in the left temporal region.

October 10, 2019 – Ultrasonography: a lymph node sized 3.7*2.4 mm, with a distinct rugged contour, and a mass lesion in the right lobe of the liver, sized 3.6*3 cm, are visualized.

Table S1: Description of clinical manifestations during application of *Karanahan***.** Patient 1.

	Positive dynamics	**No dynamics**	**Negative dynamics**
Course 1 Nov. 9, 2019			
Course 2 Nov. 28, 2019			
Dec. 2019	Residual fibrotic lesions in the left temporal region and soft tissues of the inguinal region.		
MRI, MSCT July 2, 2020	The liver parenchyma is homogeneous; no focal lesions are detected.	Several lymph nodes are detected para-aortically; the maximum long diameter of the lymph node is 10.8 mm; the minimal diameter is 4 mm. External hydrocephalus. Chronic ischemic foci are detected in the white matter in both cerebral hemispheres. A lesion 4.8 mm in diameter, with a smooth distinct contour and homogeneous structure, is visualized in the S6 segment of the right lung.	

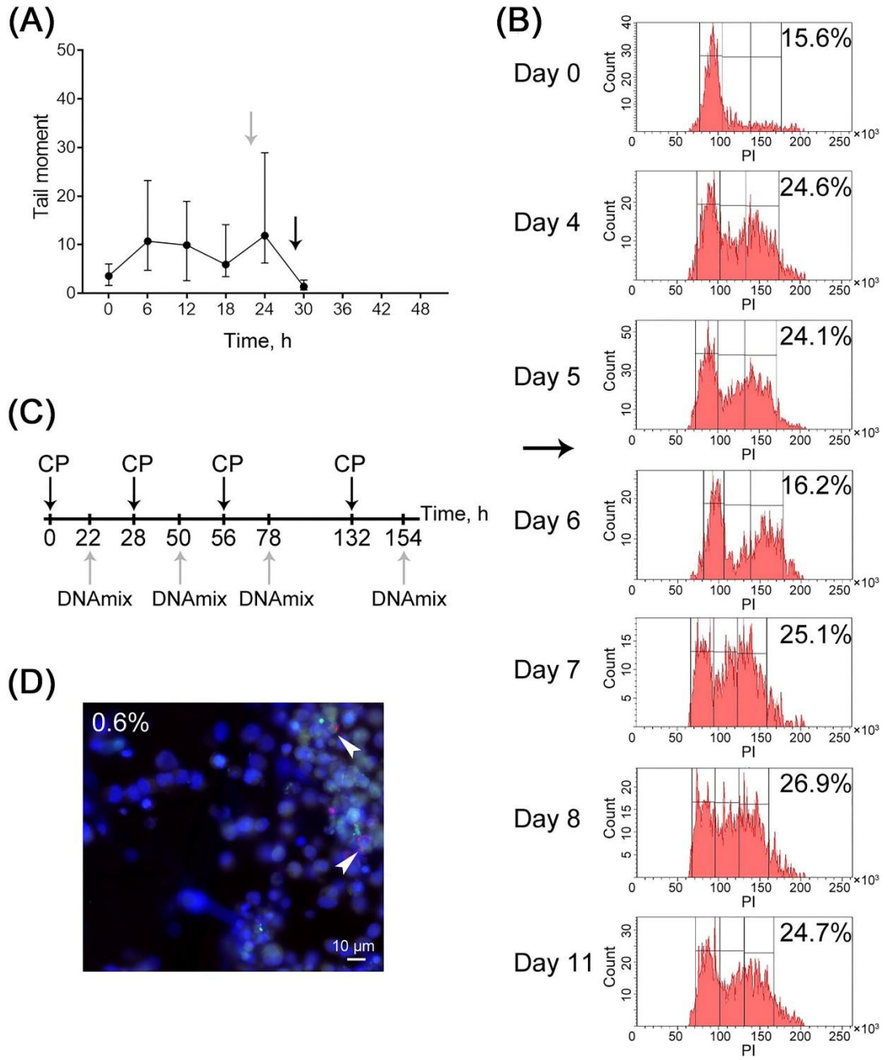

Figure S1: Patient 1: (A) DNA repair cycle in cancer cells. The medians and the 95% confidence interval for the tail moment in the comet assay are presented after different time intervals after the exposure of cells to 1 µg/mL mitomycin C are presented. The time of DNAmix administration determined for the future regimen is shown with a light gray arrow; the time of administration of a cross-linking cytostatic agent is indicated with a black arrow. (B) The cell cycle of cancer cells after three exposures to mitomycin C at an interval determined by analyzing the repair cycle; The cell cycle was quantified by flow cytometry according to propidium iodide fluorescence. The number of days after the initiation of treatment and the percentage of cells that undergo division are indicated. The black arrow shows the identified time of the fourth administration of the cytostatic cross-linking agent. (C) The resulting regimen of tumor treatment. The time of administration of CP and DNAmix is indicated. (D) Determining the number of TAMRA+ cancer stem cells. The percentage of cells is presented; arrows show examples of cancer cells internalizing the TAMRA-labeled probe.

Patient 1-2. Recurrence

Date of birth: December 28, 1960

Died in March 2024

Medical history

November 2019 – Two therapy courses using the *Karanahan* technology, complete regression of the neoplasms

March 20, 2022 – Skin induration and thickening up to 6.5 mm in the left breast is detected

September 9, 2022–October 7, 2022 – Hormone therapy with fulvestrant (N30)

November 2, 2022 – Ultrasonography: hepatomegaly, a metastasis sized 20*18*19 mm in the left liver lobe and more than six metastases sized 21–51 mm in the right lobe of the liver

November 23, 2022 – Dissection of the metastasis in the left breast

Table S2: Description of clinical manifestations during application of *Karanahan***.** Patient 1-2. Recurrence. Died in March 2024.

Positive dynamics	No dynamics	Negative dynamics
Course 1 Dec. 15, 2022		
Dec. 24, 2022	Right breast: no palpable focal abnormalities. Left breast: competent postoperative cicatrix in the upper outer quadrant and edema in the central area. Regional lymph nodes are non-palpable. Grade 1–2 edema of the left arm.	
Course 2 Jan. 12, 2023		
Jan. 21, 2022	No dynamics	
Course 3 Feb. 7, 2023		
MSCT Mar. 30, 2023, Aug. 26, 2023		Size of the neoplasms in the liver increased from 2*2 cm to 8*6 cm

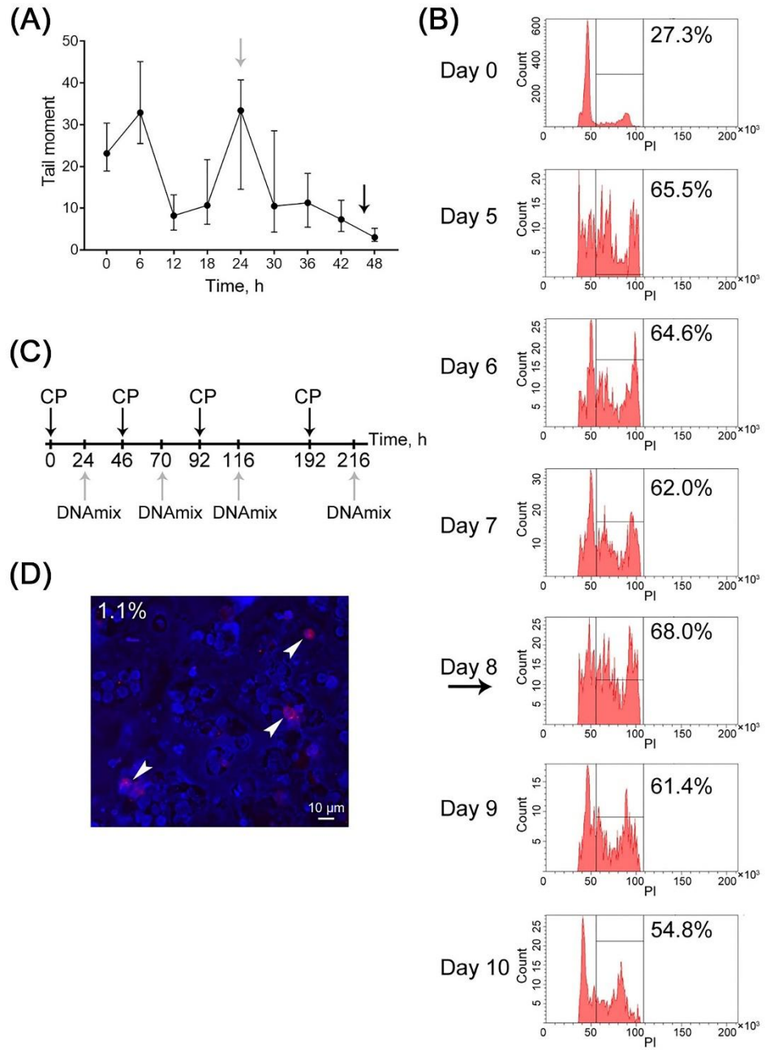

Figure S2: Patient 1-2, recurrence: (A) DNA repair cycle in cancer cells. The medians and the 95% confidence interval for the tail moment in the comet assay after different time intervals after the exposure of cells to 1 µg/mL mitomycin C are presented. The time of DNAmix administration determined for the future regimen is shown with a light gray arrow; the time of administration of a cross-linking cytostatic agent is indicated with a black arrow. (B) The cell cycle of cancer cells after three exposures to mitomycin C at an interval determined by analyzing the repair cycle; the cell cycle was quantified by flow cytometry according to propidium iodide fluorescence. The number of days after the initiation of treatment and the percentage of cells that undergo division are indicated. The black arrow shows the identified time of the fourth administration of the cytostatic cross-linking agent. (C) The resulting regimen of tumor treatment. The time of administering CP and DNAmix is indicated. (D) Determining the number of TAMRA+ cancer stem cells. The percentage of cells is presented; arrows show examples of cancer cells internalizing the TAMRA-labeled probe.

Patient 2.

Date of birth: January 19, 1971

Died in March 2020

Medical history

2019 – Synchronous bilateral breast cancer

October 7, 2019 – CT: secondary changes in the liver, foci of round and irregular shape with a rugged contour, sized up to 23 mm.

Lytic lesions of round and irregular shape with a rugged contour, sized up to 12 mm, are visualized in thoracic and lumbar vertebrae and pelvic bones.

October 11, 2019 – A tumor in the upper outer quadrant in the right breast, sized up to 3.5 cm, firm, poorly movable; a similar tumor in the left breast. In the right side of the axillary region: firm movable lymph nodes sized up to 2.5 cm. In the left side of the supraclavicular region: lymph nodes sized up to 5 mm.

October 19, 2019 – Biopsy specimens were harvested from the right-sided axillary lymph node.

November 9, 2019 – A firm poorly movable tumor sized up to 2.5 cm in the upper outer quadrant of the right breast; a similar tumor in the left breast. Regional lymph nodes are nonpalpable. In the right side of the axillary region, there is a postoperative cicatrix that appears unremarkable.

Table S3: Description of clinical manifestations during application of *Karanahan***.** Patient 2. Died in April 2020.

	Positive dynamics	**No dynamics**	**Negative dynamics**
Course 1 Nov. 9, 2019			
CT Nov. 30, 2019	Size of the necrotic region in the central area of the largest liver lesions increases. The largest lesion is sized 18 mm.	The total number of liver lesions remains unchanged.	The size of lesions in the thoracic and lumbar vertebrae and pelvic bones increases, and their number increases slightly.
Dec. 13, 2019	Left breast: a firm, poorly movable tumor, sized up to 1.5 cm, in the upper outer quadrant; no skin manifestations.		Right breast: a firm, poorly movable tumor, sized up to 4.5 cm, in the upper outer quadrant; its central zone is infiltrated.
Course 2 Dec. 13, 2019			
Jan. 9, 2020	Right breast: the tumor occupies the upper outer quadrant; swelling of the central zone persists. Left breast: a firm, poorly movable tumor, sized up to 1.0 cm, in the upper outer quadrant; no skin manifestations.		
Course 3 Jan. 9, 2019			
Feb. 16, 2020	Left breast: the tumor is not distinctly palpable.		Right breast: a firm, poorly movable tumor, sized up to 3.5 cm, in the upper outer quadrant.
Mar. 11, 2020	Right breast: a firm, poorly movable tumor, sized up to 2.0 cm, in the upper outer quadrant.		Left breast: a tumor sized 1.0 cm in the upper outer quadrant.

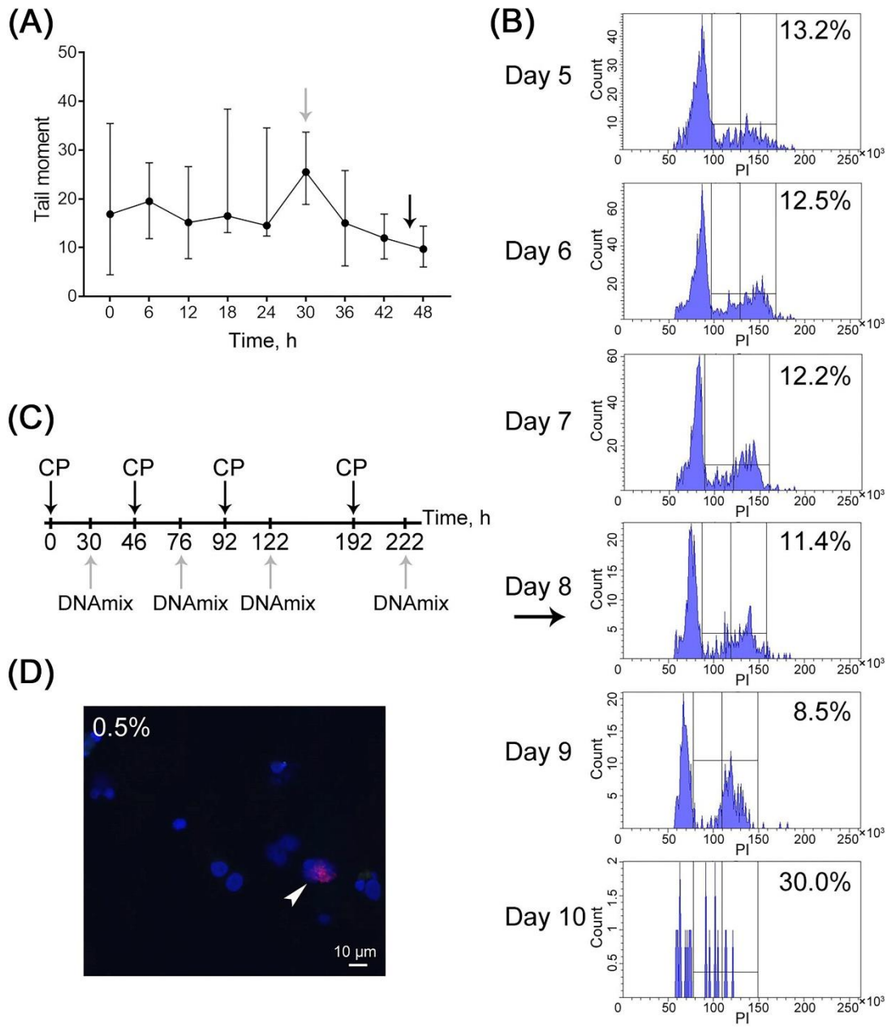

Figure S3: Patient 2: (A) DNA repair cycle in cancer cells. The medians and the 95% confidence interval for the tail moment in the comet assay after different time intervals after the exposure of cells to 1 µg/mL mitomycin C are presented. The time of DNAmix administration determined for the future regimen is shown with a light gray arrow; the time of administration of a cross-linking cytostatic agent is indicated with a black arrow. (B) The cell cycle of cancer cells after three exposures to mitomycin C at an interval determined by analyzing the repair cycle; the cell cycle was quantified by flow cytometry according to propidium iodide fluorescence. The number of days after the initiation of treatment and the percentage of cells that undergo division are indicated. The black arrow shows the identified time of the fourth administration of the cytostatic cross-linking agent. (C) The resulting regimen of tumor treatment. The time of administering CP and DNAmix is indicated. (D) Determining the number of TAMRA+ cancer stem cells. The percentage of cells is presented; arrows show examples of cancer cells internalizing the TAMRA-labeled probe.

Patient 3.

Date of birth: February 15, 1959

Died in December 2022

Medical history

2014 – Left-sided breast cancer.

2014–2017 – Left-sided radical sector resection, radiation therapy + tamoxifen

Progression, metastatic spread to skin of the anterior thorax and liver; left-sided exudative pleurisy.

2017 – Right-sided kidney cancer, right-sided nephrectomy

October 2017 – Recurrent breast cancer

Until May 10, 2018 – Administration of fulvestrant (N6), positive local dynamics (for skin metastasis and pleurisy)

Until January 2019 – Administration of fulvestrant during 13 months, negative dynamics for skin metastases

Until July 2020 – Administration of aromatase inhibitors

Dec. 8, 2020 – CT: neoplasms sized up to 12 mm along the cicatrix in the left breast. Right-sided axillary lymph nodes are enlarged to 10 mm at the borderline, left-sided lymph nodes were resected.

Left-sided thickening of the thoracic skin affecting the abdomen and multiple indurations sized up to 20*12 mm with rugged contours are visualized. Multiple foci sized up to 8 mm with distinct smooth contours are detected in the lungs. A right lower paratracheal lymph node is enlarged to 11 mm. Multiple irregularly shaped lytic and osteosclerotic lesions sized up to 25 mm, with rugged contours and the cortical layer destroyed in some regions, are visualized in thoracic vertebrae, sternum, scapulae, clavicles, humeri, and ribs. Oval and round foci with rugged contours, sized up to 35 mm, are visualized in the liver. Multiple para-aortic lymph nodes enlarged to 15 mm are detected.

Table S4: Description of clinical manifestations during application of *Karanahan*. Patient 3. Died in December 2022.

	Positive dynamics	**No dynamics**	**Negative dynamics**
Course 1 Jan. 25, 2021			
Course 2 Feb. 15, 2021			
Course 3 Mar. 5, 2021			
CT Apr. 9, 2021	Lesions sized up to 6 mm in the left breast along the cicatrix. Right axillary lymph nodes are not enlarged (size is reduced). Left-sided thickening of thoracic skin, multiple indurations up to 6 mm wide. Some foci in the lungs are not visualized; for most of them, size decreased to 2 mm. A right lower paratracheal lymph node enlarged to 8 mm. Oval and round foci, sized up to 23 mm, are visualized in the liver Multiple para-aortic lymph nodes decreased to 7 mm.	Bone foci without changes	Ground-glass opacity nodules and reticular opacities are visualized in the subpleural regions of the lower lobes of both lungs, as well as the S3 and S4 superior lobes of the left lung.
Feb. 22, 2022, Apr. 26, 2022			Progression in the liver, grade 2–3 pancytopenia

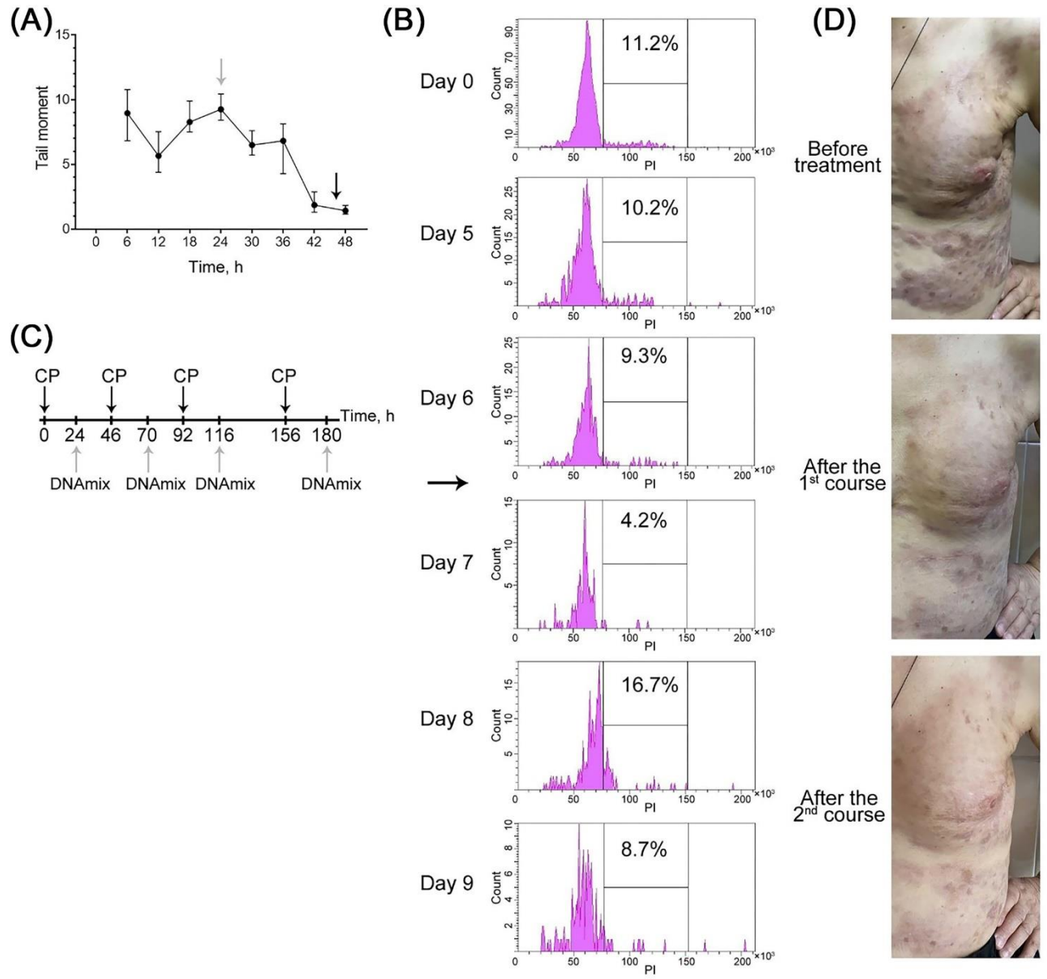

Figure S4: Patient 3: (A) DNA repair cycle in cancer cells. The medians and the 95% confidence interval for the tail moment in the comet assay after different time intervals after the exposure of cells to 1 μg/mL mitomycin C are presented. The time of DNAmix administration determined for the future regimen is shown with a light gray arrow; the time of administration of a cross-linking cytostatic agent is indicated with a black arrow. (B) The cell cycle of cancer cells after three exposures to mitomycin C at an interval determined by analyzing the repair cycle; the cell cycle was quantified by flow cytometry according to propidium iodide fluorescence. The number of days after the initiation of treatment and the percentage of cells that undergo division are indicated. The black arrow shows the identified time of the fourth administration of the cytostatic cross-linking agent. (C) The resulting regimen of tumor treatment. The time of administering CP and DNAmix is indicated. (D) Photographs of the main tumor nidi of the patient during therapy.

Patient 4.

Date of birth: October 30, 1949

Died in April 2023

Medical history

October 16, 2018 – Right-sided radical Madden mastectomy.

Histological examination: grade 2 infiltrating ductal carcinoma. Metastases spread to two lymph nodes.

Immunohistological analysis: ER 8, PR 0, HER2/neu 0, Ki67 10%.

Until 2020 – Adjuvant programmed chemotherapy (AC4 regimen), paclitaxel (N4), external beam radiation therapy, tamoxifen.

2021 – Progression.

February 10, 2021 – open biopsy from the neoplasm in the cutaneous tissue of the back and anterior abdominal wall

February 17, 2021 – Histological findings: cutaneous metastasis from breast cancer.

March 5, 2021 – Immunohistological analysis: ER 6, PR 0, HER2/neu 0, Ki67 5%.

January 23, 2021 – CT: Right breast was removed. A single calcification focus up to 5 mm in diameter is visualized in the left breast. Axillary lymph nodes are not enlarged. Ascites. Pleural cavities contain fluid with layer thickness up to 20 mm (right) and 52 mm (left) (volume up to 210 mL and 650 mL for the right and left pleural cavities, respectively). Linear pulmonary fibrosis lesions are visualized in lower lung segments. A single calcified focus sized up to 4 mm is detected in the S9 segment of the right lung. A single lesion sized 3*4 mm, most probably of fibrotic nature, is visualized in the S9 segment of the left lung. The pericardial cavity contains a small amount of fluid (up to 3 mm thick layer). Signs of numerous small osteosclerotic foci in osseous structures, sized from 1*2 mm to 7*6 mm (the largest one is detected in the right side of the 7th rib).

Table S5: Description of clinical manifestations during application of *Karanahan*. Patient 4. Died in April 2023.

Positive dynamics	No dynamics	Negative dynamics
Course 1 April 8, 2021		
Course 2 Apr. 30, 2021		
CT May 26, 2021	Fluid is visualized in the pleural cavities (layer thickness being up to 9 and 17 mm in the right and left plural cavities, respectively). No excessive fluid accumulation is found in the pericardial cavity. Multiple pathological osseous foci up to 5 mm in diameter are visualized in bones.	Ascites. Solid lesions sized 2–4 mm are visualized in the lungs (the S2 segment of the right lung; the S1-2 and S9 segments of the left lung).
Physical examination May 24, 2022		Multiple cutaneous deposits are detected at the right side within the postoperative cicatrix area and on skin. No focal pathology is observed for the left breast. No nipple discharge is detected. The regional lymph nodes are nonpalpable.
Course 3 May 24, 2021		
Physical examination Feb. 17, 2022	Cutaneous deposits are detected neither within the postoperative cicatrix area and nor on skin at the right side.	No focal pathology is observed for the left breast. No nipple discharge is detected. The regional lymph nodes are nonpalpable.	Intradermal lesions are detected within neck and the left shoulder joint on the left side.
CT Feb. 25, 2022, Feb 28, 2022	No effusion in pleural cavities.	Ascites (16 mm at the right side, 14 mm at the left side), a diffuse induration in the abdominal and retroperitoneal adipose tissue. Lung foci. Areas of radiation-induced fibrosis in the parenchyma of the upper lobe of the right lung. Interstitial changes in the basal regions of the right lung of inflammatory genesis. Mild hydropericardum (3 mm).	Capillary hepatic hemangioma (segment 4). Signs of moderate bile duct wall thickening. A single cystic-appearing lesion in the pancreatic head. Small-sized sclerotic foci 2–10 mm in diameter visualized in osseous structures (ribs, sternum, vertebral bodies, humeri, scapulae, and pelvic bones).
June 2022		Focal hepatic lesions, metastases. The patient is diagnosed with infiltrating gastric cancer.

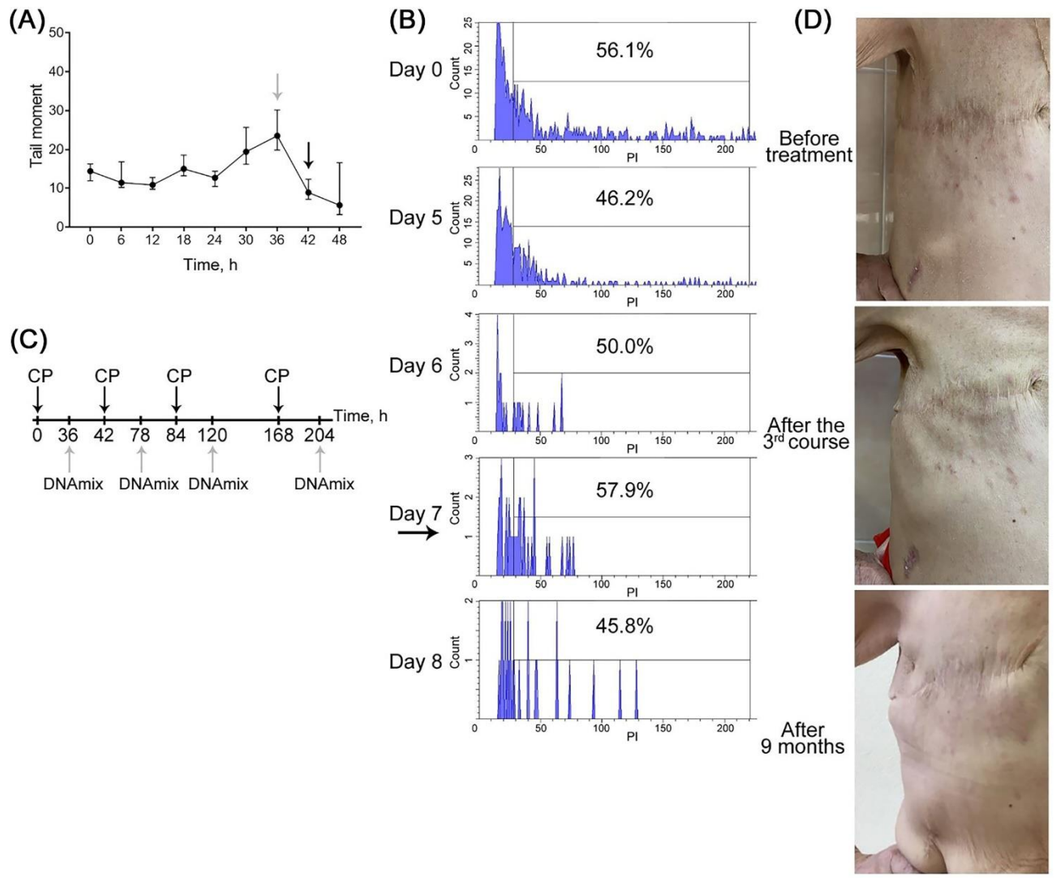

Figure S5: Patient 4: (A) DNA repair cycle in cancer cells. The medians and the 95% confidence interval for the tail moment in the comet assay after different time intervals after the exposure of cells to 1 μg/mL mitomycin C are presented. The time of DNAmix administration determined for the future regimen is shown with a light gray arrow; the time of administration of a cross-linking cytostatic agent is indicated with a black arrow. (B) The cell cycle of cancer cells after three exposures to mitomycin C at an interval determined by analyzing the repair cycle; the cell cycle was quantified by flow cytometry according to propidium iodide fluorescence. The number of days after the initiation of treatment and the percentage of cells that undergo division are indicated. The black arrow shows the identified time of the fourth administration of the cytostatic cross-linking agent. (C) The resulting regimen of tumor treatment. The time of administering CP and DNAmix is indicated. (D) Photographs of the main tumor nidi of the patient during therapy.

Patient 5.

Date of birth: May 26, 1959

Died in May 2023

Medical history

2019 – A neoplasm in the left breast was detected.

24.03.2019 – Ultrasonography: a neoplasm in the lower outer quadrant of the left breast, sized 90*52*50 mm, the lymph node is sized up to 36 mm.

March 29, 2019 – Histological findings: poorly differentiated carcinoma.

Immunohistological analysis: ER 8, PR 7, HER2/neu 2+, Ki67 40%.

Negative FISH test results.

March 26, 2019 – Skeletal scintigraphy: osteoblastic lesions in bones

April 12, 2019 – MSCT: Multiple secondary lesions in the pelvis and femoral bones

April 17, 2019 – MSCT: Multiple metastatic lesions in both lungs

April 24, 2019 – September 23, 2019 – Chemotherapy (AC8 regimen; the cumulative dose of anthracycline being 960 mg); positive dynamics for lung metastases; no changes for the osteoblastic bone metastases

October 16, 2019 – December 19, 2019 – Therapy with fulvestrant +palbociclib + bisphosphonates (N3)

January 10, 2010 – MSCT findings: bilateral pleural effusion appeared, predominantly affecting the right side.

Bilateral pleurocentesis.

January 22, 2020 – March 26, 2020 – Chemotherapy with paclitaxel (N4)

April 15, 2020 – March 2021 – Administration of aromatase inhibitors

April 8, 2021 – Cutaneous metastasis was dissected

March 20, 2021 – March 22, 2021 – CT, skeletal scintigraphy: lesions in the left breast: sized measured intramammary, 4.8 cm; subcutaneously, 3.5*2.5 cm. Skin is nonuniformly indurated to 1.5 cm. Multiple polymorphous lesions in the parenchyma of both lungs (foci sized up to 13 mm in the left lung and up to 9 mm, in the right lung). A cluster of lymph nodes (short diameter up to 15 mm) in the left axillary region. Enlarged rounded lymph nodes (n = 3) sized 10–15 mm in the mediastinal fat. The pericardial cavity contains fluid with layer thickness up to 10–12 mm. Osteosclerotic lesions in vertebrae T2 (up to 23 mm), T3 (up to 10 mm), and T7 (up to 5 mm). An osteoblastic activity focus is visualized in the T11 vertebrae (tender induration in the osseous structure without a distinct smooth contour).

Table S6: Description of clinical manifestations during application of *Karanahan*. Patient 5. Died in May 2023.

	Positive dynamics	**No dynamics**	**Negative dynamics**
Course 1 May 11, 2021			
Course 2 June 1, 2021			
Course 3 June 29, 2021			
CT Aug. 4, 2021	Reduced size of lesions in the left breast: intermammary, 3.6 cm; subcutaneously, 2.4*1.0 cm. Skin indurated nonuniformly to 0.9 cm. No new foci are identified in the lung parenchyma (S2 – 4 mm, S6 – 3 mm, S9 – 6 mm, S10 – 7 mm). A cluster of lymph nodes, with rugged contours and short diameter up to 6 mm, is detected in the left axillary region. Intrathoracic lymph nodes are not enlarged (sized up to 10 mm). Mild stranding of the mediastinal fat is detected. No excessive fluid accumulation is found in the pericardial cavity.	No dynamics for the osteosclerotic lesions in the T2, T3, and T7 vertebrae.	A moderate amount of fluid in the left pleural cavity appeared (maximum thickness, up to 12 mm). An osteosclerotic lesion in the T11 vertebra (sized up to 10 mm) is distinctly visualized.
CT Nov. 1, 2021	No pleural effusion is detected.	No significant dynamics observed for the lesions in the left breast. Short diameter of the lymph nodes is up to 7 mm; their size does not increase. No significant dynamics revealed for the bone metastases.	Size of some metastases in the lungs increases (S2 – 7.5 mm; S10 – 9 mm; no changes for other metastases).
Course 4 Nov. 24, 2021			
Nov. 4, 2021	Breast asymmetry. No pathological foci are visualized in the right breast; neither skin changes nor nipple discharge is detected. The left breast is deformed because of the tumor; two tumors, each sized up to 1.5 cm, are found in the outer quadrants. Skin of the left breast is indurated, with multiple intradermal deposits of different size (up to 2.0 cm) spreading up to the midaxillary region. Postoperative surgical margins are unremarkable. The regional lymph nodes are nonpalpable.		
Course 5 Dec. 15, 2021			
Course 6 Jan. 12, 2022			
CT Feb. 5, 2022		Two tumors are visualized in the left breast (intramammary, up to 3.6 cm; subcutaneously, up to 2.5 in the axial plane). Skin is nonuniformly indurated to 1 cm. The short diameter of axillary lymph nodes is 7–10 mm; their size does not increase. Multiple polymorphous metastases, sized 3–9 mm, are visualized in the lung parenchyma; the largest ones reside in the S2 and S10 segments of the right lung: their size and number were not changed. No significant dynamics are observed for bone metastases. Neither pleural nor pericardial effusion is detected.	

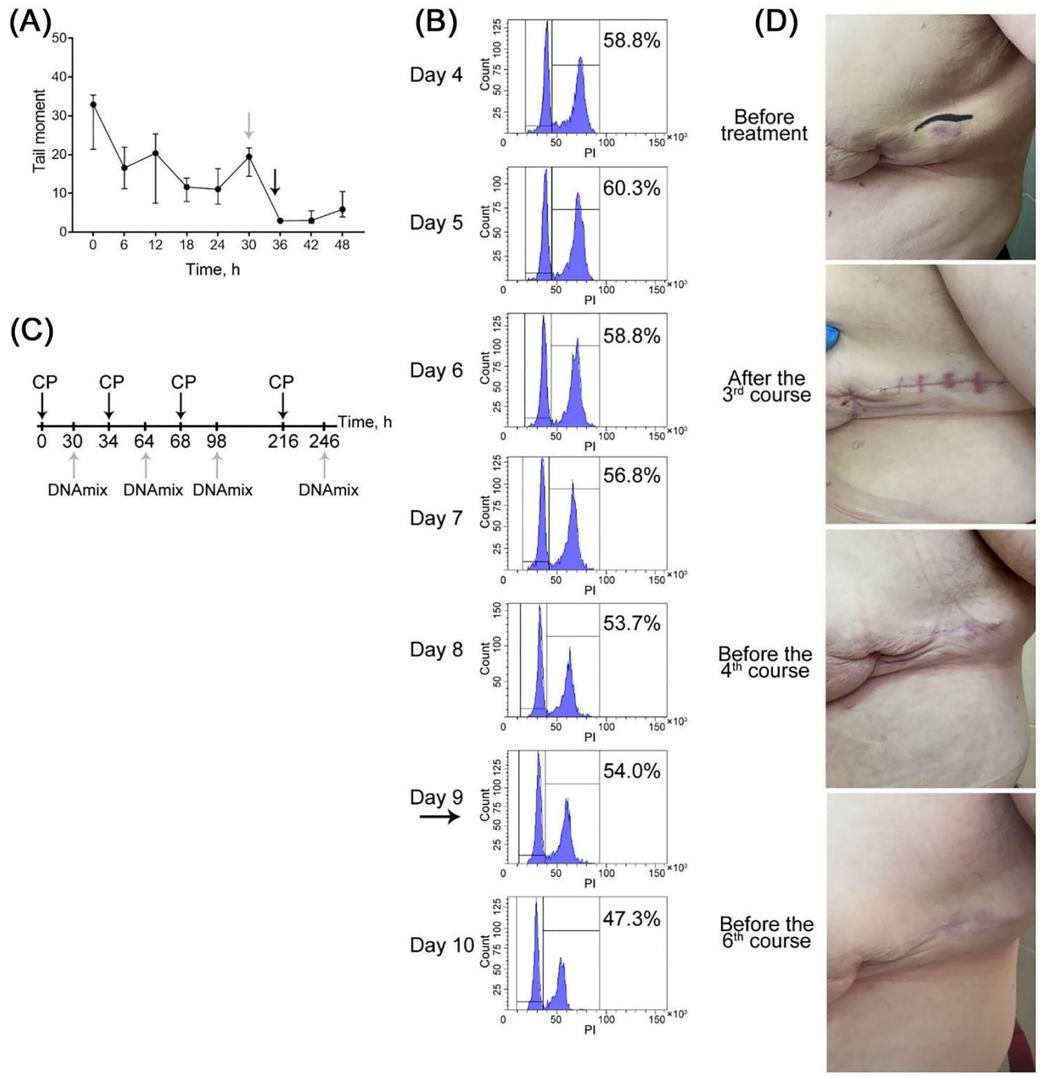

Figure S6: Patient 5: (A) DNA repair cycle in cancer cells. The medians and the 95% confidence interval for the tail moment in the comet assay after different time intervals after the exposure of cells to 1 μg/mL mitomycin C are presented. The time of DNAmix administration determined for the future regimen is shown with a light gray arrow; the time of administration of a cross-linking cytostatic agent is indicated with a black arrow. (B) The cell cycle of cancer cells after three exposures to mitomycin C at an interval determined by analyzing the repair cycle; the cell cycle was quantified by flow cytometry according to propidium iodide fluorescence. The number of days after the initiation of treatment and the percentage of cells that undergo division are indicated. The black arrow shows the identified time of the fourth administration of the cytostatic cross-linking agent. (C) The resulting regimen of tumor treatment. The time of administering CP and DNAmix is indicated. (D) Photographs of the main tumor nidi of the patient during therapy.

Patient 6.

Date of birth: July 7, 1956

Died in May 2022

Medical history

February 9, 2017 – A lump in the right breast was detected.

October 16, 2017 – Immunohistological analysis: ER 8, PR 6, HER2/neu 0, Ki67 31%.

Histological findings: grade 2 infiltrating ductal carcinoma.

October 18, 2017 – Administration of tamoxifen

February 2018 – A metastasis to soft tissues of the anterior thorax

2018–2020 – Administration of aromatase inhibitors

December 16, 2020–February 25, 2021 – Hormone therapy with fulvestrant (N4), negative local dynamics

April 2021 – June 10, 2021 – Chemotherapy (AC4 regimen), negative local dynamics

July 1, 2021 – MSCT: A lymph node sized 41*46*52 mm with a vague rugged contour is visualized in the right axillary region. Osteosclerotic lesions, up to 3.5 mm in diameter, in the T7–8 and L1 vertebrae.

July 15, 2021 – October 12, 2021 – Chemotherapy with paclitaxel (N12), negative local dynamics

October 21, 2021 – A biopsy specimen collected from the intradermal metastases of the right breast

October 11, 2021 – MSCT: Multiple small lesions in the liver with smooth and somewhat vague contours, sized 3–5.5 mm, are visualized (most likely to be cysts). No fluid accumulation in the abdominal cavity is detected. Osteosclerotic lesions are detected in the iliac wings, the L1 vertebral body and spinous processes and the S1 vertebral body.

Table S7: Description of clinical manifestations during application of *Karanahan*. Patient 6. Died in May 2022.

	Positive dynamics	No dynamics	Negative dynamics
Course 1 Nov. 16, 2021			
Nov. 25, 2021	Local inflammation and intense hyperemia in the central (perimammary) region of the right breast	Breasts D < S. No nipple discharge is detected. The upper outer quadrant of the right breast contains a poorly movable lump without a distinct contour, sized up to 7 cm, previously palpable, which cannot be convincingly identified. Several intradermal deposits are palpable at the boundary between the inner breast quadrants and on the left shoulder. No palpable lumps in the left breast are detected.	
Course 2 Dec. 7, 2021			
Dec. 16, 2021	Reduction of hyperemia in skin of the right breast, aggravation of edema at the boundary between the outer quadrants of the right breast.		
Jan. 17, 2022	Necrotic foci are detected in the nipple–areola complex.		Right breast: edema aggravation in the right-side axillary region and hyperemia; cutaneous metastases spread to the supraclavicular region. Intradermal deposits in the right-side axillary region appear. Left breast: hyperemia and an intradermal deposit in the upper inner quadrant appeared. Right-sided axillary lymphadenopathy.
Ultrasonography, MSCT Jan. 19, 2022			A lump in the right breast (skin induration at the right side, sized to 4.56 mm) with echoscopic signs of malignancy. Negative dynamics for the right-sided lymph node (size increased to 57*44*49 mm). Lung nodules along the interlobar and costal pleura, foci in the left cardiodiaphragmal corner, and parenchymal lesions in the S2 and S8 lung segments appeared. Size of the focus in S3 segment increased. Hydrothorax. A consolidated right-sided fracture of the 6th rib. Emergence of osteosclerotic lesions in the T2 and T4 vertebral bodies; the lesion in the T8 vertebral body was increased to 4.6 mm. A hepatic lesion sized 28*24*25 mm appeared.
Feb. 2022			Aggravation of patient's condition (hydrothorax and severe pain). Thoracentesis was performed twice at the chest clinic.

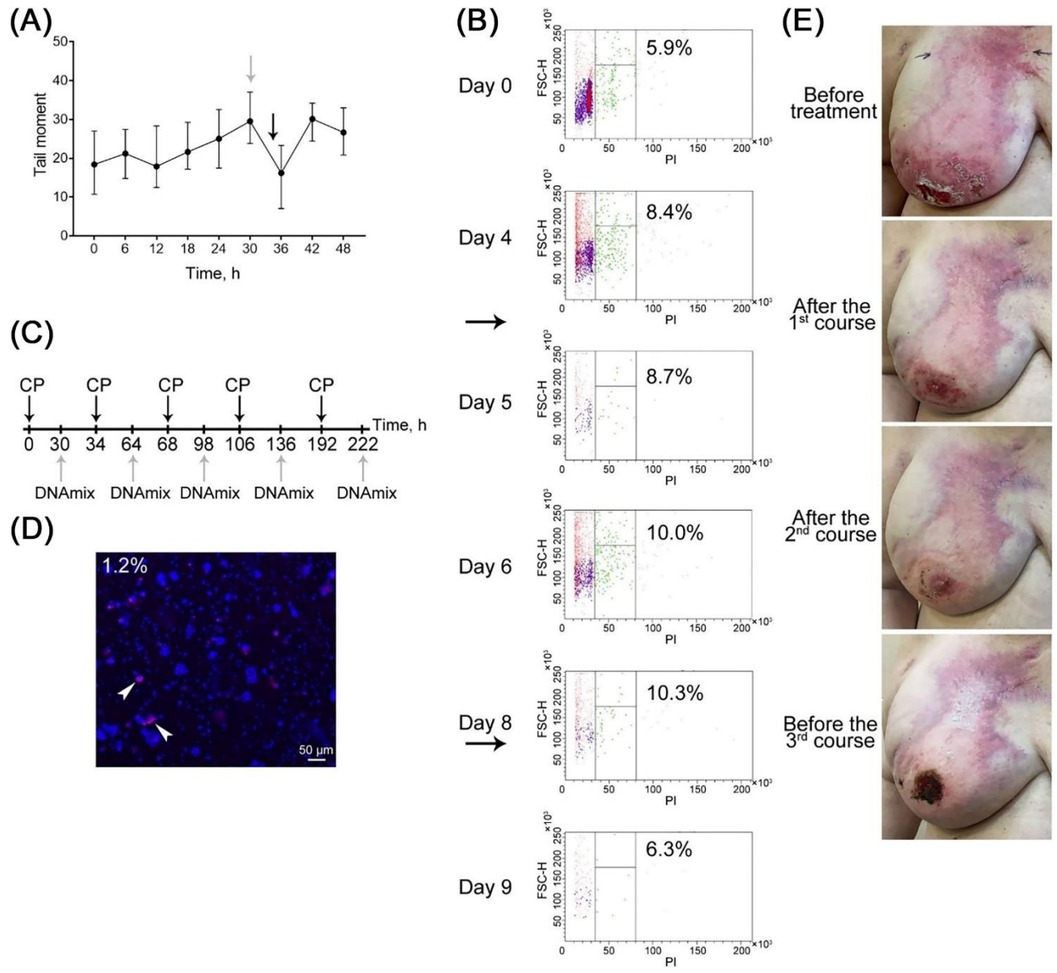

Figure S7: Patient 6: (A) DNA repair cycle in cancer cells. The medians and the 95% confidence interval for the tail moment in the comet assay after different time intervals after the exposure of cells to 1 μg/mL mitomycin C are presented. The time of DNAmix administration determined for the future regimen is shown with a light gray arrow; the time of administration of a cross-linking cytostatic agent is indicated with a black arrow. (B) The cell cycle of cancer cells after three exposures to mitomycin C at an interval determined by analyzing the repair cycle; the cell cycle was quantified by flow cytometry according to propidium iodide fluorescence. The number of days after the initiation of treatment and the percentage of cells that undergo division are indicated. The black arrow shows the identified time of the fourth administration of the cytostatic cross-linking agent. (C) The resulting regimen of tumor treatment. The time of administering CP and DNAmix is indicated. (D) Determining the number of TAMRA+ cancer stem cells. The percentage of cells is presented; arrows show examples of cancer cells internalizing the TAMRA-labeled probe. (E) Photographs of the main tumor nidi of the patient during therapy.

Patient 7.

Date of birth: March 24, 1982

Died in July 2022

Medical history

2018 – Left-sided breast cancer, T4N1M1, liver metastases

Histological findings: grade 2 infiltrating ductal carcinoma.

Immunohistological analysis: ER 0, PR 0, HER2/neu 3+.

2018-2019 – Four cycles of programmed chemotherapy (AC regimen), four cycles of monochemotherapy with docetaxel, nine injections of trastuzumab, capecitabine + trastuzumab

September 2019 – Cerebellar metastases and their surgical extirpation

January 2020 – Frontal bone metastases

2020–2021 – Chemotarget therapy (vinorelbine + trastuzumab + pertuzumab), four cycles of trastuzumab + lapatinib, six cycles of targeted therapy (Kadcyla®), chemotarget therapy (paclitaxel + trastuzumab), ten cycles of multiagent chemotarget therapy (carboplatin + Hemzar® + Herceptin®), two cycles of mono-chemotarget therapy (Halaven® + Herceptin®), 43 trastuzumab injections.

Negative dynamics observed locally and in the cerebellum; aggravation of breast edema and increased size of axillary and supraclavicular lymph nodes on the left side

March 28, 2022 – Dissection of cutaneous metastasis in the left breast

April 13, 2022 – Immunohistological analysis: ER 0, PR 0, HER2/neu 3+, Ki67 80%.

March 27, 2022 – Brain MRI: A 17*30*10 mm structure is visualized on the posterosuperior surface of the left cerebellar hemisphere. A 11*18*10 mm structure is visualized on the posterior surface of the left cerebellar hemisphere. A focal area sized 6 mm in the right occipital lobe. A focal area sized 5 mm in the lateral regions of the posterior cranial fossa along the tentorium cerebelli.

April 4, 2022 – CT: Bulky lesions in the left breast invading into the pectoral muscles on the left side (95*70 mm, 113*70 mm). Conglomerates in the infraclavicular and axillary lymph nodes on the left side (sized up to 30 mm). Nodules along the costal pleura on the left side (sized from 3 mm to 14*6.5 mm). A small cyst in the liver segment VIII; a focal steatosis area in the liver segment IVB. A solitary cyst in the right kidney.

Table S8: Description of clinical manifestations during application of *Karanahan*. Patient 7. Died in July 2022.

	Positive dynamics	**No dynamics**	**Negative dynamics**
Course 1 Apr. 19, 2022			
Course 2 May 16, 2022			
May 23, 2022	Breast hyperemia became more intense; propagation of necrotic surface in the lower quadrants of the breast.		Development of edema and hyperemia within the postoperative cicatrix (tumor tissue overgrowth).
June 6, 2022			Negative local dynamics, aggravation of breast edema and hyperemia, enlargement of lymph nodes.
Brain MRI June 6, 2022			Enlargement of lesions in the left cerebellar hemisphere (21*35 mm and 29*19 mm). Enlargement of the lesion in the right occipital lobe (11*8 mm). Enlargement of the lesion along the lateral contour of the resection cavity (12*8 mm).
CT June 16, 2022		Cysts in the liver and kidneys.	Enlargement of lumps in the left breast invading into the pectoral muscles on the left side (105*87 mm, 126*83 mm) and spreading to left shoulder muscles and intercostal muscles; marginal degeneration of the anterior segments of ribs II–V on the left side. A solid lesion next to the right margin of the body of the sternum, sized 35*27 mm, was newly detected. Enlargement of infraclavicular and axillary lymph nodes on the left side (to 35 mm). Emergence of enlarged left supraclavicular and right axillary lymph nodes. Enlargement of some focal lesions in the left lung parenchyma (from 7 to 19 mm). Effusion in the left pleural cavity.

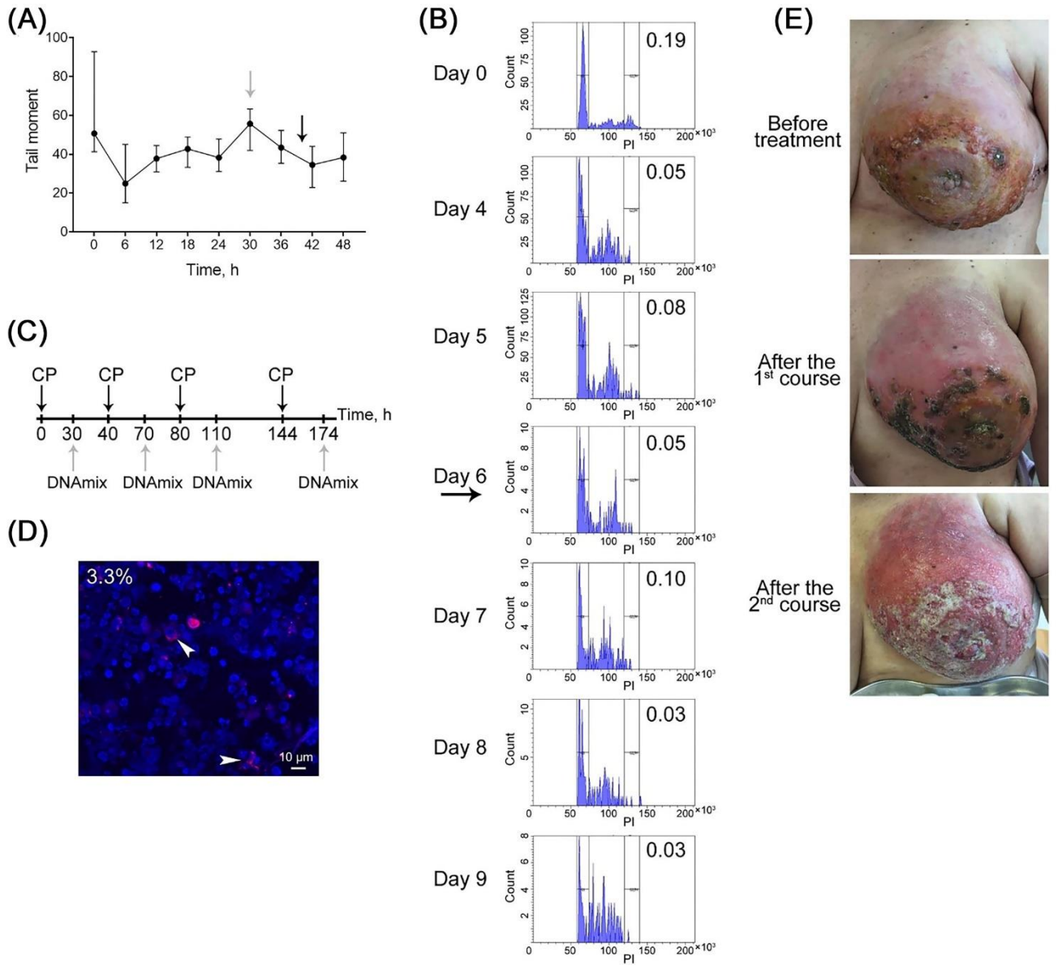

Figure S8: Patient 7: (A) DNA repair cycle in cancer cells. The medians and the 95% confidence interval for the tail moment in the comet assay after different time intervals after the exposure of cells to 1 µg/mL mitomycin C are presented. The time of DNAmix administration determined for the future regimen is shown with a light gray arrow; the time of administration of a cross-linking cytostatic agent is indicated with a black arrow. (B) The cell cycle of cancer cells after three exposures to mitomycin C at an interval determined by analyzing the repair cycle; the cell cycle was quantified by flow cytometry according to propidium iodide fluorescence. The number of days after the initiation of treatment and the ratio between the percentage of cells undergoing division in the G2/M phase and the percentage of cells in the G1 phase are indicated. The black arrow shows the identified time of the fourth administration of the cytostatic cross-linking agent. (C) The resulting regimen of tumor treatment. The time of administering CP and DNAmix is indicated. (D) Determining the number of TAMRA+ cancer stem cells. The percentage of cells is presented; arrows show examples of cancer cells internalizing the TAMRA-labeled probe. (E) Photographs of the main tumor nidi of the patient during therapy.

Patient 8.

Date of birth: January 5, 1950

Died in June 2022

Medical history

February 2021 – Left-sided breast cancer

June 11, 2021 – Immunohistological analysis: ER 0, PR 0, HER2/neu 1+, Ki67 70-75%.

2021 – Four courses of multiagent chemotherapy (AC regimen), four courses of second-line multiagent chemotherapy (135 mg docetaxel).

March 31, 2022 – Open biopsy from the intradermal metastasis

April 18, 2022 – Immunohistological analysis: ER 0, PR 0, HER2/neu 0, Ki67 27%.

April 27, 2022 – Breast ultrasonography: a stellate-shaped homogeneous lesion sized 21*18*21 mm, with a distinct rugged contour; skin infiltration up to 9.7 mm thick above the lesion.

April 26, 2022 – MRI: secondary bone cancer. CT signs of acute hepatitis, but no data proving secondary liver cancer have been obtained. Multiple simple liver cysts. Signs of liver cysts in both kidneys. A pancreatic cyst. Local right-sided induration of fat of the mesoileum. Bilateral hydrothorax.

Table S9: Description of clinical manifestations during application of *Karanahan*. Patient 8. Died in June 2022.

	Positive dynamics	**No dynamics**	**Negative dynamics**
Course 1 Apr. 20, 2022			
Course 2 May 16, 2022			
May 19, 2022	Hyperemia on the breast surface became less intense.	No changes in the wound surface were observed.	

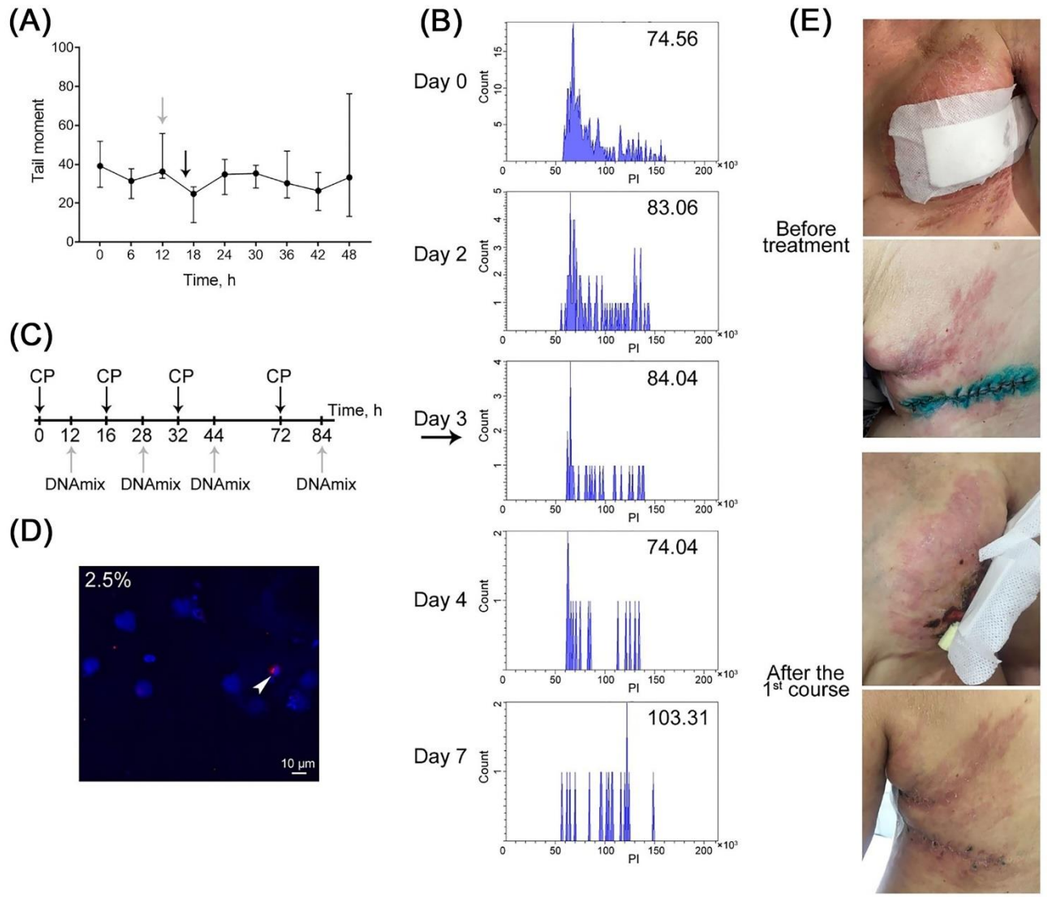

Figure S9: Patient 8: (A) DNA repair cycle in cancer cells. The medians and the 95% confidence interval for the tail moment in the comet assay after different time intervals after the exposure of cells to 1 μg/mL mitomycin C are presented. The time of DNAmix administration determined for the future regimen is shown with a light gray arrow; the time of administration of a cross-linking cytostatic agent is indicated with a black arrow. (B) The cell cycle of cancer cells after three exposures to mitomycin C at an interval determined by analyzing the repair cycle; the cell cycle was quantified by flow cytometry according to propidium iodide fluorescence. The number of days after the initiation of treatment and the median percentage of cells exhibiting propidium iodide fluorescence are indicated. The black arrow shows the identified time of the fourth administration of the cytostatic cross-linking agent. (C) The resulting regimen of tumor treatment. The time of administering CP and DNAmix is indicated. (D) Determining the number of TAMRA+ cancer stem cells. The percentage of cells is presented; arrows show examples of cancer cells internalizing the TAMRA-labeled probe. (E) Photographs of the main tumor nidi of the patient during therapy.

Patient 9.

Date of birth: February 21, 1962

Died in August 2023

Medical history

2022 – The patient discovered a lump in the right breast, but did not seek medical treatment. In February 2022, abrupt tumor progression started: the tumor size increased and ulceration developed. The patient sought medical treatment in Autumn 2022 and was diagnosed with right-sided breast cancer (breast adenocarcinoma according to the fine-needle aspiration biopsy data).

February 27, 2023 – Immunohistological analysis: ER 8, PR 7, HER2/neu 0, Ki67 40%.

March 1, 2023 – Grade 2 invasive breast carcinoma (no special type), Nottingham histological grading score 7 (3+3+1).

January 30, 2023: CT: A tumor in the right breast. Right axillary lymph nodes enlarged (to 23*20 mm); multiple focal pulmonary lesions; a focal liver lesion (26*22 mm). No enlarged lymph nodes in the mediastinum are detected.

Table S10. Description of clinical manifestations during application of *Karanahan*. Patient 9. Died in August 2023.

	Positive dynamics	No dynamics	Negative dynamics
Course 1 Mar. 03, 2023			
Course 2 Apr. 04, 2023			
Apr. 2023	No focal lesions are detected in the left breast by palpation. The right breast is deformed by the tumor, tuberous, having extensive ulceration areas. A lymph node sized up to 3*4 cm is palpable in the right supraclavicular region. Grade 1–2 edema of the right arm. Positive dynamics for the condition of the local tumor; tumor edges are well-conditioned; the size of tissue decay areas became smaller, the ichorous odor subsided.		
Course 3 June 2, 23			
June 2023	No focal lesions are detected in the left breast by palpation. The right breast is deformed by the tumor, tuberous, has smaller size; the ulceration areas are partially epithelialized.	A lymph node sized up to 3*4 cm is palpable in the right supraclavicular region. Grade 2 edema of the right arm.	
Course 4 Aug. 16, 2023			
Aug. 2023	No focal lesions are detected in the left breast by palpation. The right breast is deformed by the tumor, tuberous, has smaller size; the ulceration areas are partially epithelialized.	A lymph node sized up to 3*4 cm is palpable in the right supraclavicular region. Grade 2 edema of the right arm.	The therapy course was discontinued because of abrupt deterioration of patient's condition and aggravation of the multiple organ dysfunction syndrome. The patient was transferred to the intensive care unit.

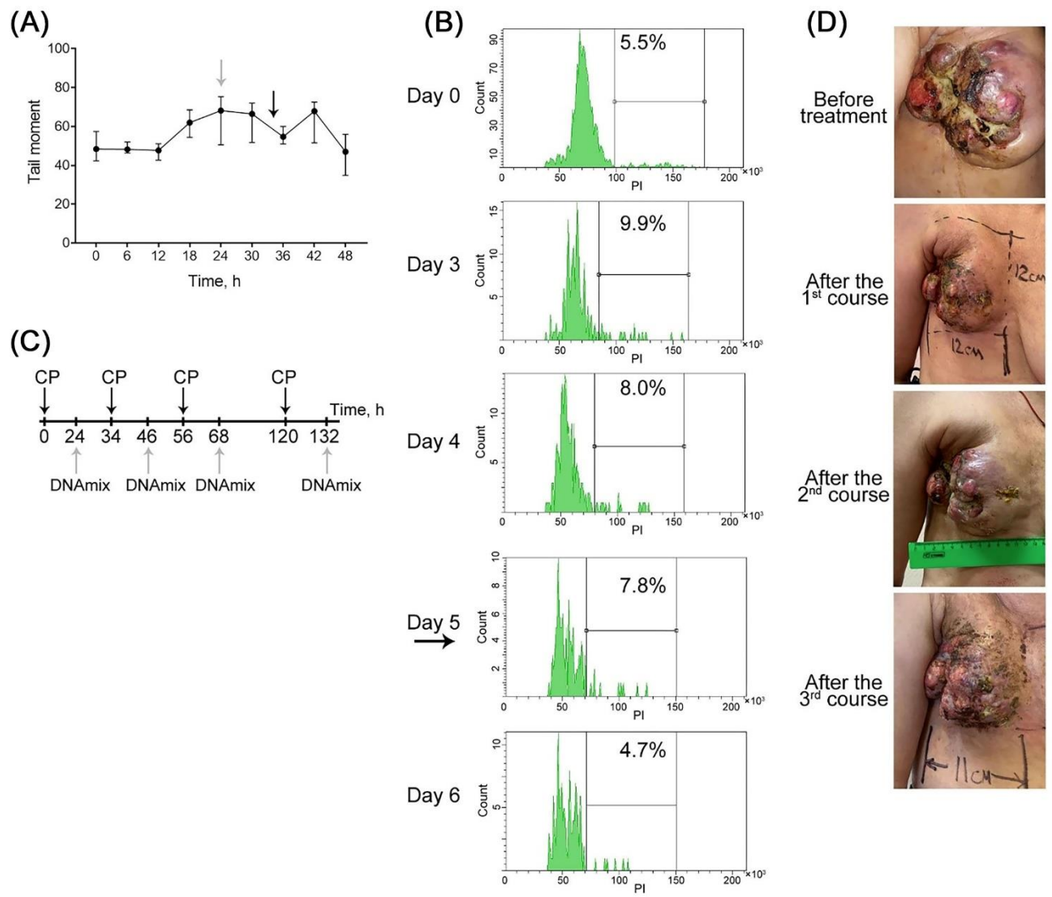

Figure S10: Patient 9: (A) DNA repair cycle in cancer cells. The medians and the 95% confidence interval for the tail moment in the comet assay after different time intervals after the exposure of cells to 1 μg/mL mitomycin C are presented. The time of DNAmix administration determined for the future regimen is shown with a light gray arrow; the time of administration of a cross-linking cytostatic agent is indicated with a black arrow. (B) The cell cycle of cancer cells after three exposures to mitomycin C at an interval determined by analyzing the repair cycle; the cell cycle was quantified by flow cytometry according to propidium iodide fluorescence. The number of days after the initiation of treatment and the percentage of cells that undergo division are indicated. The black arrow shows the identified time of the fourth administration of the cytostatic cross-linking agent. (C) The resulting regimen of tumor treatment. The time of administering CP and DNAmix is indicated. (D) Photographs of the main tumor nidi of the patient during therapy.

Patient 10.

Date of birth: July 4, 1971

Medical history

2017 – A malignant neoplasm in the right breast.

February 23, 2017 – Histological findings: grade 2 infiltrating ductal carcinoma.

April 3, 2017 – Immunohistological analysis: ER 6, PR 4, Ki67 27%.

Four courses of neoadjuvant multiagent chemotherapy (AC regimen).

August 25, 2017 – Right-sided radical Madden mastectomy with simultaneous breast reconstruction using TRAM flap.

October 5, 2017– Histological findings: complete therapeutic pathomorphosis (grade 4); no tumor growth in the lymph nodes was detected.

Until January 2019 – Administration of tamoxifen 20 mg/day

Progression

August 10, 2018 – Ultrasonography: right supraclavicular lymph nodes sized up to 10*10 mm and 5*5 mm.

August 23, 2018 – Open biopsy from the right supraclavicular lymph nodes.

January 30, 2019 – March 2019 – Administration of aromatase inhibitors

Negative dynamics.

March 20, 2018 – Multiagent chemotherapy (AC4 regimen), followed by targeted hormone therapy.

July 26, 2019 – MSCT of the neck: signs of scarce lymph nodes in the infraclavicular, jugular, and deep cervical regions.

August 21, 2019 – September 17, 2019 – A palliative course of external beam radiation therapy for lymph nodes.

October 15, 2019 – Immunohistological analysis: ER 8, PR 8, Ki67 20–25%.

October 18, 2019 – April 5, 2020 – Administration of fulvestrant (N7).

May 2021 – MRI of the neck: secondary lesions in the supraclavicular lymph node at the right side; a nodule in the right lobe of the thyroid gland.

July 28, 2021 – Abdominal ultrasound: a hepatic lesion sized 9*8 mm (a region affected by liver disease? Hemangioma?).

Capecitabine (6 months)

December 22, 2022 – Ultrasonography: supraclavicular lymph nodes at the right side are enlarged (maximum size, 25*19 mm)

Until May 14, 2022 – Eleven doses of paclitaxel (the 12^{th} course was not performed because of the abnormal blood chemistry test results).

May 25, 2022 – Contrast-enhanced CT of soft-tissue structures of the neck: enlarged cervical lymph nodes at the right side (levels Ia and IIa); secondary cancer cannot be ruled out. Isolated indurations in the supraclavicular lymph nodes at the right side without signs of pathological neovascularization are visualized.

December 8, 2022 – CT of soft-tissue structures of the neck: a nodule in the soft tissues of the supraclavicular region at the right side; hyperplasia of cervical and supraclavicular lymph nodes.

March 1, 2023 – Gemcitabine + carboplatin.

May 15, 2023 – Histological examination: intradermal metastasis of adenocarcinoma

Table S11: Description of clinical manifestations during application of *Karanahan*. Patient 10.

	Positive dynamics	No dynamics	Negative dynamics
Course 1 May 25, 2023			
June 2023		Lymphedema of the right upper limb; the right breast reconstructed using a flap, appears unremarkable. A fistula sized up to 4*2 cm in the axillary region. A nonmovable hard cyanotic lymph node, up to 2 cm in diameter, in the supraclavicular region.	
Course 2 June 2, 2023			
June 2023	The ulceration area within the intradermal metastasis is reduced (less intense hyperemia and smaller size).	Lymphedema of the right upper limb; the right breast reconstructed using a flap. A persisting fistula sized up to 3*2 cm in the axillary region. Cytologic evaluation detected no atypical cells. A nonmovable hard cyanotic lymph node, up to 2 cm in diameter, in the supraclavicular region.	
Course 3 July 26, 2023			

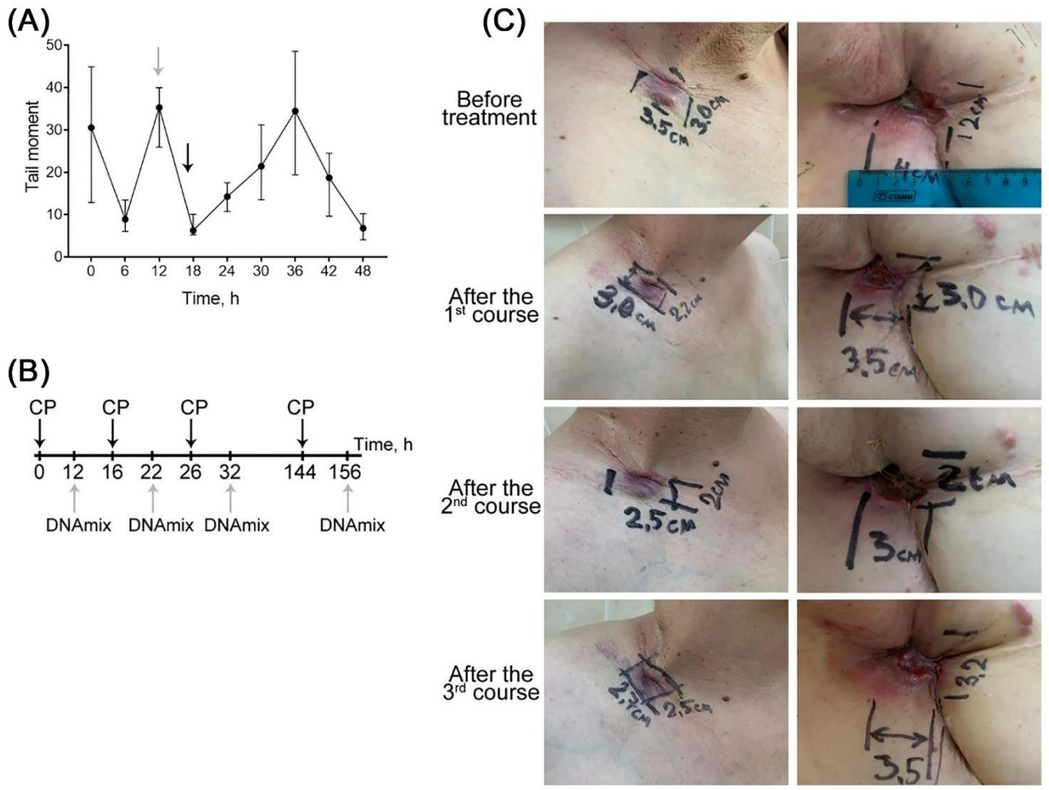

Figure S11: Patient 10: (A) DNA repair cycle in cancer cells. The medians and the 95% confidence interval for the tail moment in the comet assay after different time intervals after the exposure of cells to 1 μg/mL mitomycin C are presented. The time of DNAmix administration determined for the future regimen is shown with a light gray arrow; the time of administration of a cross-linking cytostatic agent is indicated with a black arrow. (B) The resulting regimen of tumor treatment. The time of administering CP and DNAmix is indicated. (C) Photographs of the main tumor nidi of the patient during therapy.

Patient 11.

Date of birth: August 15, 1975

Medical history

2014 – Left-sided radical Madden mastectomy

Six courses of multiagent chemotherapy.

Breast reconstruction using TRAM flap. External beam radiation therapy was not performed. Administration of tamoxifen during 1 year.

2018 – Excision of a chest wall metastasis.

Administration of aromatase inhibitors and luteinizing hormone–releasing hormone agonists.

09.01.2018 – Ultrasonography: diffuse lesions in the liver and the pancreas.

Administration of aromatase inhibitors and luteinizing hormone–releasing hormone agonists (Zoladex).

November 9, 2020 – Ultrasonography: an endometrial polyp, a retention cyst in the right ovary

2021 – Laparoscopic ovariectomy; ovarian cysts detected by histological examination.

January 16, 2023 – MSCT: a 51*41*35 mm lesion in the S8/10 segments of the left lung; fluid in the right pleural cavity (layer thickness, 25 mm); a conglomerate of bronchopulmonary lymph nodes (29*23 mm).

Table S12: Description of clinical manifestations during application of *Karanahan*. Patient 11.

	Positive dynamics	No dynamics	Negative dynamics
Course 1 May 25, 2023			
Course 2 June 2, 2023			
June 2023	Reduced lesion size.	No palpable lumps in breasts are detected. Regional lymph nodes are not distinctly palpable. A round painless lesion in the right suprascapular area is palpable.	The therapy course was discontinued; the patient was withdrawn from the study due to health reasons.

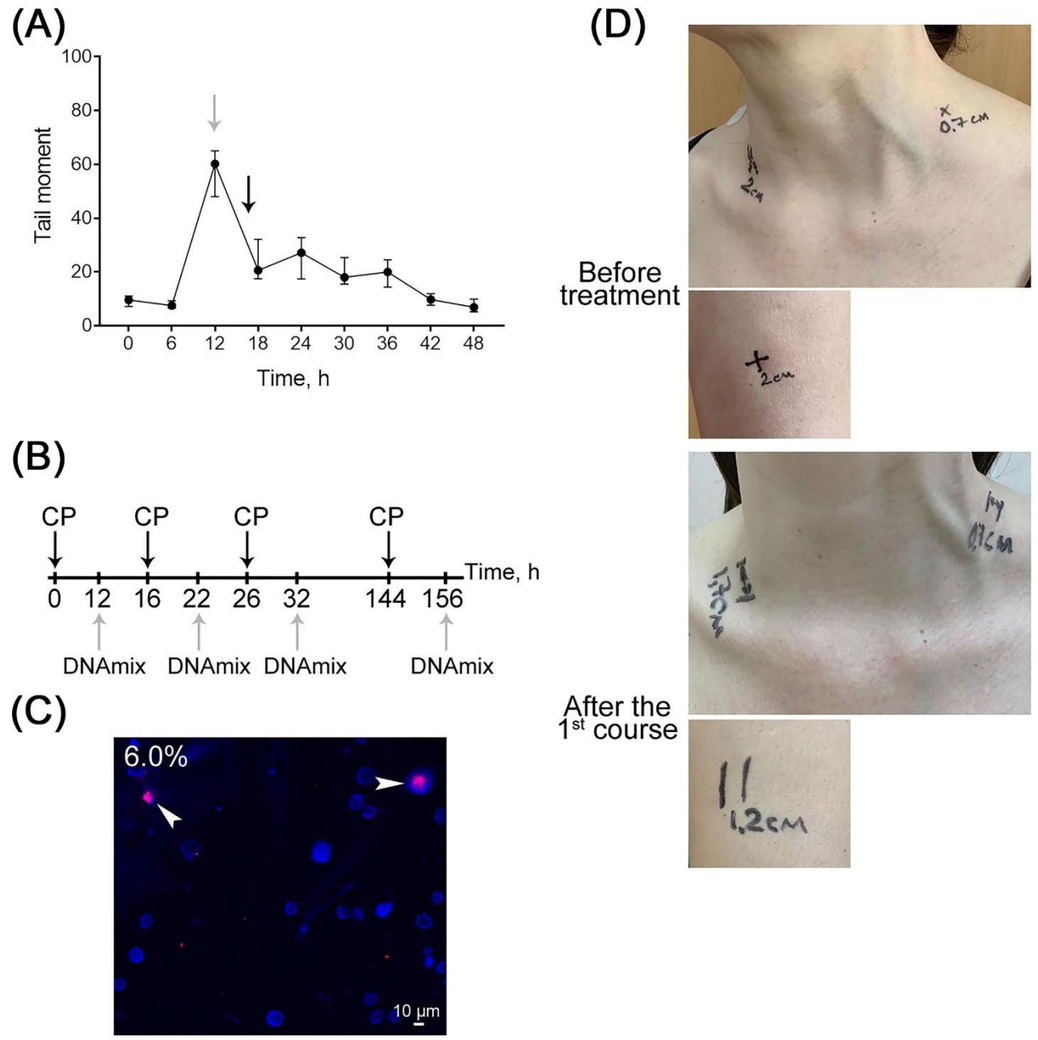

Figure S12: Patient 11: (A) DNA repair cycle in cancer cells. The medians and the 95% confidence interval for the tail moment in the comet assay after different time intervals after the exposure of cells to 1 μg/mL mitomycin C are presented. The time of DNAmix administration determined for the future regimen is shown with a light gray arrow; the time of administration of a cross-linking cytostatic agent is indicated with a black arrow. (B) The resulting regimen of tumor treatment. The time of administering CP and DNAmix is indicated. (C) Determining the number of TAMRA+ cancer stem cells. The percentage of cells is presented; arrows show examples of cancer cells internalizing the TAMRA-labeled probe. (D) Photographs of the main tumor nidi of the patient during therapy.

Patient 12.

Date of birth: April 8, 1976

Medical history

2018 – HER-positive breast cancer.

Three cycles of neoadjuvant multiagent chemotherapy (AC regimen)

Three cycles of docetaxel + trastuzumab therapy.

April 2023 – The patient developed cough at rest, exertional dyspnea, breast edema and discomfort.

April 25, 2023 – MSCT: bilateral hydrothorax.

Histological examination: grade 2 infiltrating ductal carcinoma.

Immunohistological analysis: ER 8, PR 8, HER2/neu 3+, Ki67 75%.

Secondary lesions in the lungs and intrathoracic lymph nodes; bilateral metastatic pleurisy.

May 23, 2023 – Right-sided thoracocentesis. A breast cancer metastasis (metastatic adenocarcinoma) was verified cytologically.

Table S13: Description of clinical manifestations during application of *Karanahan*. Patient 12**.**

Positive dynamics	No dynamics	Negative dynamics
Course 1 June 2, 2023		
June 2023	Mild hyperemia of the central zone of the left breast; the tumor contour is not distinctly palpable because of edema. Edema of the central zone of the right breast. The tumor contour is vaguely palpable in the upper outer quadrant (diameter being ~ 3 cm). Intradermal deposits disseminated throughout breast skin are also palpable. Regional axillary and left supraclavicular lymph nodes (hard, partially movable and painless, sized up to 1.5 cm in diameter) are palpable.	
Course 2 July 26, 2023		
Course 3 Aug. 12, 2023		
Course 4 Sept. 11, 2023		
Sept. 2023	Reduced edema severity for both breasts.	The tumor contour is vaguely palpable in the upper outer quadrant (diameter being ~ 3 cm). Intradermal deposits disseminated throughout breast skin are also palpable. Regional axillary and left supraclavicular lymph nodes (hard, partially movable and painless, sized up to 1.5 cm in diameter) are palpable.
Course 5 Oct. 9, 2023		
Oct. 2023	Reduced rate of plural effusion accumulation and fluid volume; less intense dyspnea.	

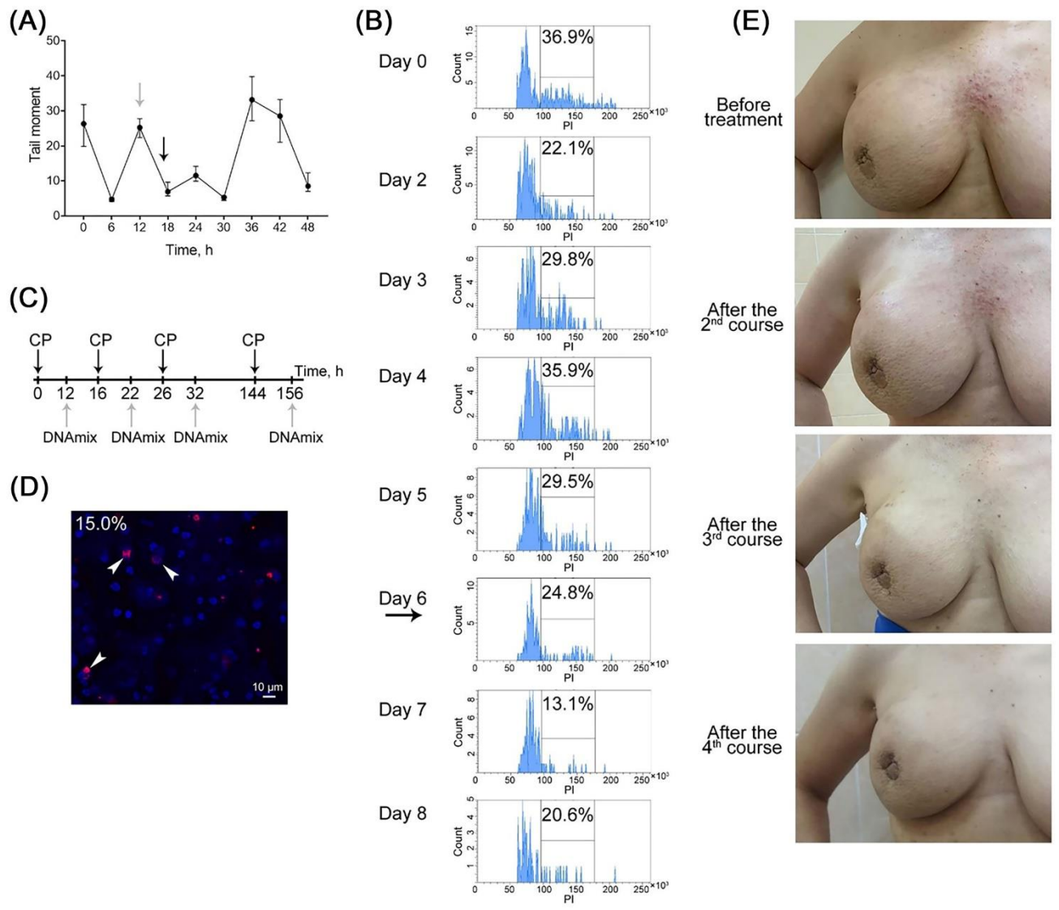

Figure S13: Patient 12: (A) DNA repair cycle in cancer cells. The medians and the 95% confidence interval for the tail moment in the comet assay after different time intervals after the exposure of cells to 1 μg/mL mitomycin C are presented. The time of DNAmix administration determined for the future regimen is shown with a light gray arrow; the time of administration of a cross-linking cytostatic agent is indicated with a black arrow. (B) The cell cycle of cancer cells after three exposures to mitomycin C at an interval determined by analyzing the repair cycle; the cell cycle was quantified by flow cytometry according to propidium iodide fluorescence. The number of days after the initiation of treatment and the median percentage of cells exhibiting propidium iodide fluorescence are indicated. The black arrow shows the identified time of the fourth administration of the cytostatic cross-linking agent. (C) The resulting regimen of tumor treatment. The time of administering CP and DNAmix is indicated. (D) Determining the number of TAMRA+ cancer stem cells. The percentage of cells is presented; arrows show examples of cancer cells internalizing the TAMRA-labeled probe. (E) Photographs of the main tumor nidi of the patient during therapy.